Proc. Natl. Acad. Sci. USA
Vol. 87, pp. 3378–3382, May 1990
Biochemistry

Topography of toxin-acetylcholine receptor complexes by using photoactivatable toxin derivatives

B. CHATRENET*, O. TRÉMEAU†, F. BONTEMS†, M. P. GOELDNER*, C. G. HIRTH*, AND A. MÉNEZ†

*Laboratoire de Chimie Bio-organique, Centre National de la Recherche Scientifique Unité Associée 1386, Université Louis Pasteur, Strasbourg, Faculté de Pharmacie, BP 24, 67401 Illkirch-Graffenstaden, France; and †Service de Biochimie, Département de Biologie et Laboratoire d'Ingénierie des Protéines, Centre d'Etudes Nucléaires Saclay, 91191 Gif-sur-Yvette Cedex, France

Communicated by Jean-Marie Lehn, October 18, 1989 (received for review May 25, 1989)

ABSTRACT **We have defined the molecular environment of a snake neurotoxin interacting with the high- and low-affinity binding sites of the nicotinic acetylcholine receptor (AcChoR). This was done by photocoupling reactions using three toxin derivatives with photoactivatable moieties on Lys-15, Lys-47, and Lys-51. Competition data showed that Lys-47 belongs to the toxin-AcChoR interacting domain whereas the other two residues are excluded from it. We first tentatively determined the threshold of covalent coupling, indicative of the proximity between the photoactivatable probes and subunits, by quantifying the coupling occurring between the same derivatives and a model compound (i.e., a toxin-specific monoclonal antibody). We then (*i*) quantified the coupling yields occurring when both binding sites of AcChoR were occupied by the toxin derivatives, (*ii*) discriminately quantified the coupling yields at the high-affinity binding site, and (*iii*) deduced the coupling yields at the low-affinity binding site. In the high-affinity site, the probes on Lys-15 and Lys-47 predominantly reacted with the high-affinity site of the AcChoR α subunit whereas the probe on Lys-51 reacted with the δ subunit. In the low-affinity site, the probe on Lys-47 predominantly reacted with the low-affinity site of the α chain and the β chain whereas those on Lys-15 and Lys-51 reacted with the γ and δ chains, respectively. A three-dimensional model showing a unique organization of AcChoR bound to two toxin molecules is presented.**

Determination of protein–protein interactions is one of the most challenging issues in biology. Interacting domains can be identified by chemical modifications of selected residues. Such techniques have proven suitable for delineating functionally critical residues of curaremimetic toxins from snake venoms (1–11). The domain by which toxin-α, a neurotoxin present in venom of the spitting cobra *Naja nigricollis* (12), interacts with the nicotinic acetylcholine receptor (AcChoR) was first predicted from comparison of analogous sequences. This prediction was supported by chemical modification studies (2). Understanding of the molecular mechanisms associated with the postsynaptic blocking ability of toxin-α now requires identification of the AcChoR subunits that directly interact with or are in proximity to the bound toxin.

It is well documented that one AcChoR oligomer is composed of five subunits (2α, β, γ, and δ) and has two toxin binding sites (13). We discriminately quantified the yield of light-induced coupling occurring at the low- and high-affinity binding sites, between each of the five subunits of the receptor and three radioactive toxin derivatives bearing a photoactivatable arylazido probe on a single lysine residue. To facilitate interpretation of our results, we performed, in parallel, a similar experiment using a model compound [i.e., a toxin-specific monoclonal antibody (8, 14)] that displays a high affinity for the toxin but has only a single class of toxin binding site and two different subunits. Data obtained with the monoclonal antibody proved of great help in interpreting our results obtained with the more complex pentameric AcChoR (13). The toxin derivatives chosen for this study had their probes located at Lys-15 and Lys-47 because they belong, respectively, to the region interacting with the antibody and AcChoR and at Lys-51 because it is excluded from both interacting domains (2, 8, 10). The data obtained led us to propose a model depicting the environment of the toxin complexed to the high-affinity and low-affinity binding sites of AcChoR.

MATERIALS AND METHODS

HPLC columns C_{18} μBondapak were purchased from Waters. Toxin-α from *N. nigricollis* was prepared from venom as described (12). *Torpedo marmorata* AcChoR-rich membranes were purified according to Saitoh *et al.* (15). The monoclonal antibody (Mα1) was prepared and purified according to Boulain *et al.* (8). The concentration of toxin-α binding sites was determined using [^{3}H]toxin-α as a radioactive tracer. All other chemicals were of the purest grade commercially available.

The preparation and characterization of photoactivatable derivatives will be published in detail elsewhere. Briefly, 1 μmol of [^{3}H]toxin-α (3 Ci/mmol; 1 Ci = 37 GBq) in 0.5 ml of 0.05 M sodium phosphate (pH 7) was incubated with 3 μmol of *p*-azidobenzoyl *N*-hydroxysuccinimide ester in 0.5 ml of acetonitrile for 3 hr at room temperature (10). The toxin derivatives were separated from excess reagent by filtration through Bio-Gel P-2 (1 cm × 18 cm) equilibrated in 10% (vol/vol) acetic acid and fractionated on a C_{18} reversed-phase HPLC column. Four major radioactive fractions were resolved. Their molar extinction coefficient determined at 280 nm indicated that 1 mol of reagent was incorporated per mol of toxin. The modified amino acid residue was identified by tryptic mapping of the carboxymethylated toxin derivatives. The three derivatives modified on Lys-15, Lys-47, and Lys-51 were used in the present study.

Binding affinities of the derivatized toxins for AcChoR (3.2 nM) and Mα1 (7 nM) were determined by competition against [^{3}H]toxin-α (1.25–13 nM; 15–37 Ci/mmol), according to Faure *et al.* (2). Apparent equilibrium dissociation constants were calculated according to Ishikawa *et al.* (16). For toxin-antibody cross-linking studies, a 0.2-ml quartz cell and 1-mm optical path was used with a 200-W Hg lamp (OSRAM-HBO). Mα1 (200 pmol) was incubated in the dark with 300 pmol of ^{3}H-labeled monomodified derivative in a final volume of 0.09 ml of 0.05 M sodium phosphate (pH 7.2) containing 0.077 M NaCl, for 1 hr at room temperature. Under these conditions, 75% of the toxin binding sites were occupied in Mα1. The sample was then irradiated for 30 min at 4°C. In a control

The publication costs of this article were defrayed in part by page charge payment. This article must therefore be hereby marked "*advertisement*" in accordance with 18 U.S.C. §1734 solely to indicate this fact.

Abbreviation: AcChoR, acetylcholine receptor.

experiment, a 100-fold molar excess of native toxin was preincubated for 1 hr with the antibody prior to addition of the photoactivatable tritiated toxin. The mixture was then treated as described below. The same results were obtained using the irradiation conditions described below for AcChoR.

The AcChoR–toxin complexes were irradiated at 10°C, in a 1-ml UV cell (1-cm optical path). Routinely, 100 pmol of AcChoR binding sites was incubated with 150 pmol of monomodified toxin-α in a 0.5 ml of 50 mM sodium phosphate, pH 7.2/0.15 M NaCl. After a 2-hr incubation in the dark at room temperature, the sample was irradiated at 305 nm for 30 min.

We prepared the complex having its high-affinity binding site preferentially occupied by the photoactivatable derivative by (*i*) incubating AcChoR-rich membranes containing 450 pmol of toxin-α binding sites with 350 pmol of modified toxin-α for 2 hr at room temperature in a final volume of 1.5 ml and then (*ii*) adding 4.5 nmol of native toxin-α (13-fold excess) at 4°C in the presence of EDTA (2 mM) for 72 hr. Under these conditions, ≈45% of toxin-α binding sites remained occupied by the modified toxin.

$NaDodSO_4$/PAGE was performed by the method of Laemmli using slab gels with a thickness of 1 mm or 1.6 mm (17).

After irradiation, the antibody-toxin complexes were immediately heated at 100°C for 3 min in 0.1 M dithiothreitol. The running and stacking gels contained 0.1 M dithiothreitol and 11% and 6% acrylamide, respectively. Protein staining was performed using 0.15% Coomassie brillant blue in 45% (vol/vol) methanol/10% (vol/vol) acetic acid for 1 hr. For quantitative determination of radioactivity, the gel was cut into 1-mm slices and each slice was placed in a glass scintillation vial containing 90% (vol/vol) Lipoluma, 8% (vol/vol) Lumasolve, and 2% (vol/vol) water and was heated for 3 hr at 60°C before radioactivity was measured.

After irradiation, the suspension of AcChoR-rich membranes was either dialyzed against four 1-liter changes of 10 mM sodium phosphate, pH 7.2/2 mM EDTA or used directly. Samples of 50–100 μg of protein were incubated for 2 hr at room temperature with 2% (wt/vol) $NaDodSO_4$/1.2 mM dithiothreitol before electrophoresis. The running and stacking gels contained 10% and 5% polyacrylamide, respectively. Protein staining and quantitative determination of radioactivity in the gel were performed as above.

RESULTS

Binding Affinities of Photoactivatable Toxin-α Derivatives. Table 1 shows the dissociation constants of the complexes formed between Mα1 or AcChoR and toxin derivatives modified on Lys-15, Lys-47, or Lys-51. In agreement with previous data (2, 6, 8, 10), we observed that (*i*) modification of Lys-15 decreased the affinity of toxin-α for Mα1, (*ii*) modification of Lys-47 induced a decrease in affinity for AcChoR, and (*iii*) modification of Lys-51 did not alter the toxin affinity for either target.

Table 1. Equilibrium dissociation constants of complexes formed between three photoactivatable toxin-α derivatives and AcChoR or monoclonal antibody Mα1

Modified residue	K_d, nM	
	AcChoR	Mα1
None	0.02 ± 0.01	0.4 ± 0.1
Lys-15	0.02 ± 0.01	2.5 ± 0.2
Lys-47	0.12 ± 0.02	0.4 ± 0.1
Lys-51	0.02 ± 0.01	0.5 ± 0.1

Values are deduced from competition experiments between [^{3}H]toxin-α (9 nM to 13 nM) and various concentrations of each derivative toward AcChoR (3.2 nM toxin-α binding site) or Mα1 (7 nM) according to Ishikawa *et al.* (16).

Specific Cross-Linking Between Photoactivatable Toxin-α Derivatives and Mα1. The free [^{3}H]toxin (7 kDa) and the light (20 kDa) and heavy (52 kDa) chains of Mα1 can be readily separated by $NaDodSO_4$/PAGE (18). Upon irradiation of the photoactivatable [^{3}H]toxin-Mα1 complexes, we found a single new radioactive band migrating with an apparent molecular mass of 59 kDa, as expected for the heavy chain-toxin complex. This irreversible coupling was specific since it vanished after preincubation of Mα1 with an excess of unlabeled toxin-α whereas it was unaffected with an excess of the homologous but non-cross-reacting (8) erabutoxin b. Quantification of specific cross-linking between Mα1 and modified toxins is shown in Table 2. Irrespective of the position of the probe, coupling occurred exclusively at the Mα1 heavy chain and the highest reaction yield was obtained with the Lys-15-modified toxin derivative.

Specific Cross-Linking Between Photoactivatable Toxin Derivatives and AcChoR from *T. marmorata*. $NaDodSO_4$/PAGE profiles of radioactivity obtained after light-induced coupling between ^{3}H-labeled toxin derivatives and AcChoR are presented in Fig. 1. We found three or four radioactive bands migrating with apparent molecular masses of 47 kDa, 57 kDa, 67 kDa, and 74 kDa. They correspond to complexes between [^{3}H]toxin derivatives and the α, β, γ, and δ subunits, respectively, assuming that each receptor subunit-toxin adduct has an apparent molecular mass equal to the sum of the apparent masses of α (40 kDa), β (50 kDa), γ (60 kDa), or δ (67 kDa) chains and toxin-α (7 kDa). Similar radioactive patterns were obtained using gel electrophoresis under reducing and nonreducing conditions (data not shown). Under nonreducing conditions, only the apparent molecular mass value of δ chain-toxin complex changed, migrating as a dimer (140 kDa). The irreversible coupling to AcChoR was specific since (*i*) no labeling was detected in the dark, (*ii*) no radioactivity was incorporated upon irradiation using nonderivatized [^{3}H]-toxin-α, and (*iii*) preincubation with a 10-fold molar excess unlabeled toxin-α abolished the coupling (Fig. 1*D*).

Upon irradiation, 5%, 11%, and 9% of the receptor-toxin complexes obtained, respectively, with derivatives modified at Lys-15, Lys-47, and Lys-51 were found to form a covalent bond between the toxin and the receptor. The three patterns of radioactivity bound to AcChoR subunits were different (Table 3). These data are analyzed in the *Discussion*.

Dissociation kinetics of the AcChoR-derivatized toxin complexes were biphasic, indicating that despite the presence of the probe, each derivative could distinguish between the high- and low-affinity binding sites (19–22). The two toxin-binding sites were discriminated by treating the fully saturated receptor-derivative complexes with a 10-fold molar excess of unlabeled native toxin for 72 hr. The high-affinity binding site was thus predominantly occupied by ^{3}H-labeled photoactivatable toxin derivative whereas the other site was occupied by native toxin. Table 4 shows the extent of

Table 2. Yield of cross-linking between lysine-modified photoactivatable [^{3}H]toxin-α and Mα1

Modified residue	% radioactivity	
	Heavy chain	Light chain
None	0	0
Lys-15	10 ± 0.5	0
Lys-47	2 ± 0.5	0
Lys-51	1 ± 0.1	0

A derivative (300 pmol) was irradiated for 30 min with 200 pmol of Mα1. The sample was submitted to $NaDodSO_4$/PAGE. Radioactivity was measured in 1-mm gel slices. The ratio of radioactivity incorporated in the heavy and light chains to the radioactivity layered on the gel was expressed as percent.

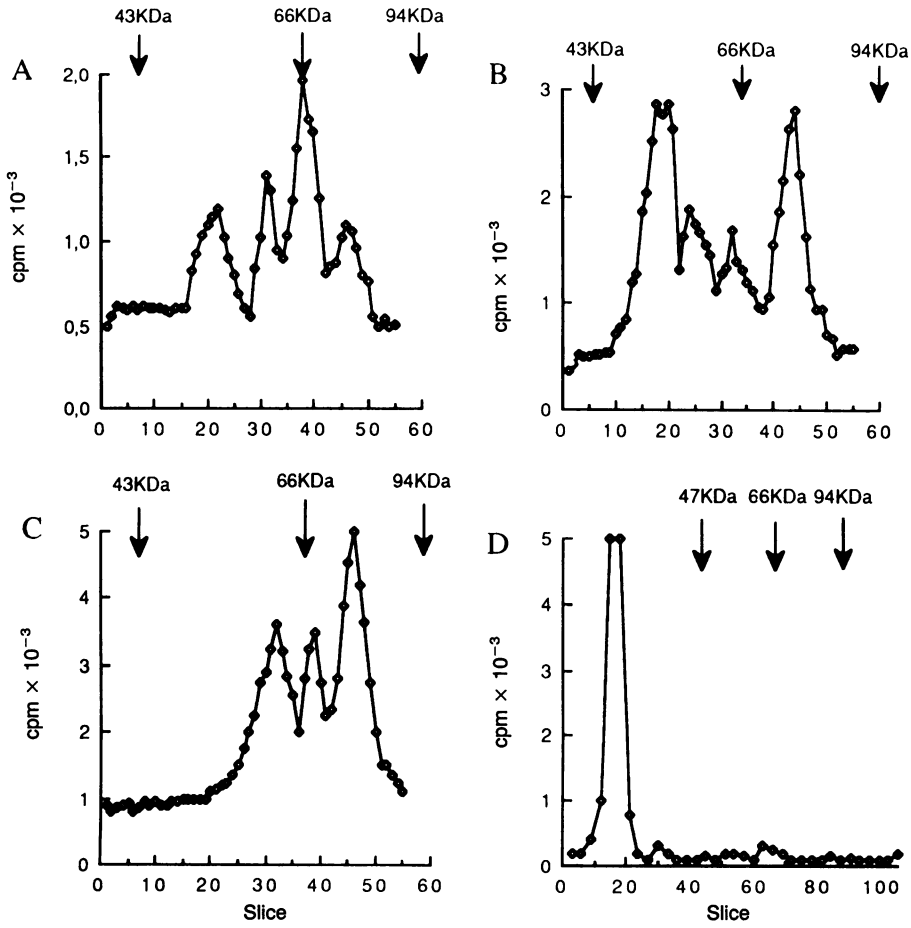

FIG. 1. $NaDodSO_4$/PAGE radioactive profile of *T. marmorata* AcChoR-rich membranes (100 pmol of toxin-α binding sites) irradiated in the presence of [^{3}H]-toxin-azido derivatives (150 pmol; 3 Ci/mmol), modified at Lys-15 (*A*), Lys-47 (*B*), Lys-51 (*C*). (*D*) Control experiment in which the receptor was preincubated with a 10-molar excess of unlabeled toxin-α before being irradiated in the presence of Lys-47-modified derivative. In all cases the receptor occupancy was maximal. The amount of complexes layered on the gels was equal to 170, 285, 255, 150 pmol in *A*, *B*, *C*, and *D*, respectively. Radioactivity in 1-mm gel slices was measured. (*A* and *B*) Four radioactive bands migrating at 47 kDa, 57 kDa, 67 kDa, and 74 kDa are shown. (*C*) We only observed three radioactive bands at 57 kDa, 67 kDa, and 74 kDa, indicating the absence of labeling between the α subunit of the AcChoR and the monomodified toxin-α at Lys-51. (*D*) Inhibition of covalent labeling by an excess of native toxin-α.

radioactivity incorporated into each subunit, after irradiation, in the high-affinity binding site. Differences between these results and those in Table 3 reflected the extent of coupling at the low-affinity binding site (Table 4). Analysis of these data is presented in the *Discussion*.

DISCUSSION

We have probed the molecular environment of a cobra neurotoxin bound to a monoclonal immunoglobulin (Mα1) and to the high- and low-affinity toxin binding sites of the AcChoR. This was achieved using three toxin derivatives bearing a photoactivatable moiety on a single identified lysine residue, located at position 15, 47, or 51. As inferred from crystallographic data of analogous proteins (for review, see refs. 1, 3, and 4), the polypeptide chain of toxin-α from *N. nigricollis* is folded in three adjacent loops forming a large β-sheet surface to $\approx$500 Å^2. Lys-15 and Lys-47 belong, respectively, to the first and third loops and are on the concave side of the sheet, both side chains pointing in the same direction. In contrast, Lys-51, which belongs to the third loop, is located on the convex face and points in the opposite direction. Previous works showed that modification of Lys-47 and Lys-15 resulted in a decrease in affinity for AcChoR and Mα1, respectively, whereas modification of Lys-51 had no effect toward either complex formation (2, 6, 8, 10). The present data agreed with these findings, further confirming that Lys-15 and Lys-47 belong, respectively, to the binding domain with Mα1 and AcChoR whereas Lys-51 is excluded from both sites.

Formation of covalent bonds using photoactivatable probes required both low chemical selectivity of the activated probe and spatial proximity between the probe and residues of Mα1 or AcChoR. From simple geometrical considerations, we estimated that a *p*-azidobenzoyl group, linked to a lysine side chain, probed a dome emerging above the toxin surface with a radius of $\approx$6 Å. Cross-linking occurred only when complexes were formed since (*i*) it vanished when Mα1 or AcChoR were preincubated with an excess of nonderivatized toxin; (*ii*) estimated rates of covalent bond formation with nitrene ($k = 10^3$–10^6 $M^{-1}\cdot s^{-1}$) or with their rearranged azacycloheptatetraenes ($k > 10^3$ $M^{-1}\cdot s^{-1}$ with amino groups) are

Table 3. Overall cross-linking between derivatized toxin-α and AcChoR

Modified toxin-α residue	% toxin-α receptor complex covalently linked after irradiation	Distribution of radioactivity among receptor subunits, %			
		α	β	γ	δ
Lys-15	5	1.3 ± 0.1	0.8 ± 0.1	2.2 ± 0.2	0.9 ± 0.2
Lys-47	11	4.4 ± 0.5	2.0 ± 0.6	1.7 ± 0.4	2.9 ± 0.7
Lys-51	9	0	3.1 ± 0.4	1.7 ± 0.3	4.1 ± 0.5

Radioactive complex (mixture of covalent and noncovalent complexes) was treated as in Fig. 1. All the radioactivity incorporated in the gel (bound to the four subunits) was measured. The percentage of covalent complex formation was expressed as the ratio of incorporated radioactivity to the total radioactivity layered on the gel (column 2). Columns 3, 4, 5, and 6 show the percentage of the radioactivity distributed on subunits α, β, γ, and δ, respectively ($n = 5$).

Table 4. Distribution of cross-linking on the different subunits at the high- and low-affinity binding sites of AcChoR

Modified toxin-α residue	Toxin-α binding site on AcChoR occupied	% toxin-α receptor complex covalently linked after irradiation	Distribution of radioactivity among receptor subunits, %			
			α	β	γ	δ
Lys-15	HA	5	2.8 ± 0.3	0.7 ± 0.1	0.7 ± 0.2	0.9 ± 0.2
	LA		0	0.9	3.6	0.9
Lys-47	HA	11	5.8 ± 0.2	1.2 ± 0.4	1.3 ± 0.4	3.0 ± 0.6
	LA		3.0	2.7	2.3	2.8
Lys-51	HA	9	0	1.6 ± 0.1	1.7 ± 0.1	5.7 ± 0.1
	LA		0	4.7	1.7	2.4

Values were calculated from data obtained by $NaDodSO_4$/PAGE (Fig. 1). HA, high affinity; LA, low affinity. Column 3 indicates the yield of total radioactivity specifically bound to all four subunits. Columns 4, 5, 6, and 7 indicate the percentage of the total radioactivity specifically incorporated on α, β, γ, and δ subunits. The values of the low-affinity binding site cross-linking were deduced from (HA + LA) and (HA) experimental results.

several orders of magnitude higher than the dissociation rates of the toxin-AcChoR ($k < 1 \times 10^{-5}\ M^{-1}$) and toxin-Mα1 ($k < 1 \times 10^{-2}\ M^{-1}$) complexes. However, the experiments did not provide information about events occurring in the millisecond time scale, including rapid conformational changes within complexes or intramolecular reactions within the toxin. Cross-linking patterns may reflect all these phenomena.

We first met difficulties in interpretating the coupling data resulting from reactions between derivatized toxins and the pentameric AcChoR (see Table 4). To clarify this situation, we examined the data for the light-induced coupling between the same photoactivatable derivatives and a model compound—i.e., a monoclonal antibody (Mα1). This compound was chosen because (*i*) it has a high affinity for the toxin (8), (*ii*) it possesses a single class of toxin binding sites (8), (*iii*) it has only two different subunits, and (*iv*) like other antigen–antibody complexes (23), it interacts with the toxin by well-defined contacts (8). Moreover, upon irradiation, the toxin-Mα1 and toxin-AcChoR complexes have similar low-coupling yields (<11%), which might reflect, in both cases, nitrene reactivity, toxin intramolecular reactions, or both, as suggested in other instances (24). Strikingly, coupling to Mα1 exclusively occurred with the heavy subunit. The probe on Lys-15 displayed the highest coupling yield further confirming the antigenic role of this residue (8) and indicating that the loop 1 of toxin-α is in proximity to the Mα1 heavy chain. Previous data have shown that neither the adjacent loop 2 [i.e., Tyr-25, Lys-27, and Trp-29 (8, 10)] nor the still more remote loop 3 (i.e., Lys-47 and Lys-51) belong to the epitope recognized by Mα1 (refs. 8 and 10 and this work). Nevertheless, the photoactivatable probes at Lys-47 and Lys-51 showed a slight (i.e., 1 ± 0.5% and 2 ± 0.5%, respectively) but reproducible coupling. We, therefore, concluded that under these experimental conditions any coupling yield equal to or lower than 2.5% may not necessarily reflect a close proximity between the probe and an interacting macromolecule. This value was then taken as a reasonable threshold in the analysis of the toxin-AcChoR covalent complexes.

Electron microscopy studies indicated that the two structurally nonequivalent (19–22) toxin binding sites of AcChoR are oriented at about 140° to one another (25), and biochemical data showed that they encompass, at least partially, the two α subunits (26, 27). Previous cross-linking studies established that AcChoR was composed of α, β, γ, and δ subunits (28–33) and also depicted an organization of the subunits within the receptor alone (32) or bound to a toxin (33). We have now described the environment of a toxin molecule bound at the high- and low-affinity binding sites and deduced a unique organization of the five subunits of AcChoR.

Two series of coupling experiments were undertaken. (*i*) Both sites were simultaneously occupied by a photoactivatable derivative. (*ii*) The high-affinity binding site was preferentially occupied by a photoactivatable derivative whereas the other site was predominantly occupied by native toxin. Since the procedure used to favor this differential occupancy was based on competition experiments using an excess of native toxin, the two populations were not completely homogeneous and the resulting data were contaminated by a slight contribution of labeling at the low-affinity binding site. The covalent coupling pattern occurring at the low-affinity site was deduced by substracting the coupling data resulting from experiments performed when only the high-affinity site was occupied by the derivatized toxin, from data obtained when both the high- and low-affinity sites were occupied by the same derivative. Our data were analyzed by considering that (*i*) only one α chain is implicated in each binding site (13), (*ii*) the two α chains are not adjacent (13), (*iii*) only the highest coupling yields above 2.5% are of significance (see above), (*iv*) a derivative bound to an AcChoR molecule does not react with another receptor molecule since the same cross-linking pattern was found using solubilized or membrane receptor, treated or not at pH 11 (data not shown), and (*v*) like other analogous toxins (1, 3, 4), toxin α has two sides, the concave side being probed by the derivatives modified at Lys-15 and Lys-47, at the edges of loop 1 and loop 3, respectively, and the convex side being probed by Lys-51 on loop 3.

When both sites were simultaneously occupied by derivatives, the highest coupling yields occurred with probes at Lys-47 (11%) and Lys-51 (9%), suggesting that loop 3 is embedded in the complex, probably in the central pit of the receptor (34). Also, the probe at Lys-51 did not react with either α chain, indicating that the convex side of the toxin is remote from these subunits, in both the high- and low-affinity binding sites. Since each α chain bears a toxin binding site (13), our data support the view that the convex face of the toxin is not implicated in recognition with the receptor (1, 3, 4). In contrast, the probe at Lys-51 reacted with the β (3.1%) and δ (4.1%) chains, suggesting that the convex side faces them, at least at one site. The situation became clearer when the two sites were discriminated. In the high-affinity site the probes on Lys-47 (5.8% coupling) and Lys-15 (2.8% coupling) both reacted with the high-affinity sites on the α chain whereas the probe at Lys-51 (5.7% coupling) reacted with the δ chain. In its high affinity site, most of the concave side of the toxin is facing the α chain whereas its convex side, at least at the level of loop 3, is facing the δ chain. This implies that the δ chain is on the right of the high-affinity site of the α chain. The situation at the low-affinity binding site was somewhat different. The probes on Lys-15 and Lys-51 reacted, respectively, with the γ (3.6% coupling) and β (4.7% coupling) chains. These data indicated that (*i*) the convex side at loop 3 is facing the β chain, implying that this subunit is on the right of the low-affinity site of the α chain; (*ii*) the concave site on loop 1 is in proximity to the γ chain, i.e., on the left of the bound toxin and hence on the left of the α chain bearing the low-affinity site. Results obtained with Lys-47-modified toxin were more difficult to interpret since the four subunits

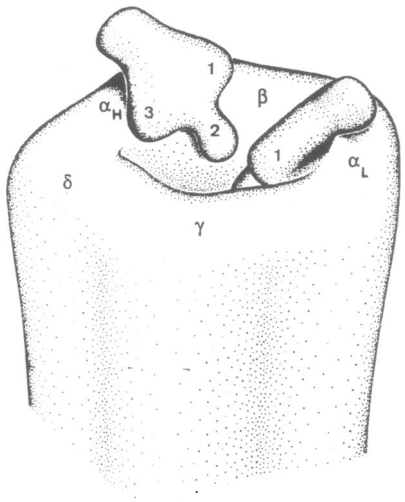

FIG. 2. Tentative represention of nicotinic AcChoR complexed with two snake toxin molecules. The receptor part was redrawn from data of Brisson and Unwin (34) and the envelope of the toxin was deduced from the crystallographic structure of the homologous erabutoxin b (11). The toxin bound to the high-affinity binding site is seen from the back, with loops 1, 2, and 3 from right to left in front of the viewer, whereas the toxin bound to the low-affinity binding site is seen from the edge of loop 1. Each toxin molecule binds to one of the two α subunits. The β subunit is flanked by the two α subunits and the γ subunit is located to the front with the δ chain on the left. Although the two toxin molecules bind to the receptor with different affinities, no difference in their respective representation has been made. The two molecules are assumed to occupy a symmetrical position with the loop 3 being embedded into the central pit and the loop 1 emerging at the surface of the receptor and, therefore, an inclination of about 20° was given to toxin molecules.

were nearly equally labeled. This can be the consequence of the intertwining of the subunits and/or of the mobility of the toxin bound to the low-affinity site (10). Thus, the five subunits have been independently probed at both the high- and low-affinity binding sites, favoring a unique arrangement around the receptor pseudoaxis of symmetry and depicting a different environment of this toxin bound at the two sites (Fig. 2). In this model, the two molecules were assumed to occupy a symmetrical position, with the most highly reacting loop 3 being embedded into the central pit and the less-reacting loop 1 emerging at the surface of the receptor. Since both loops 1 and 3 are facing the high-affinity site of the α chain, an inclination of about 20° was given to the molecule. As a result, loop 2 is also mostly in contact with this subunit, in agreement with chemical (1–5) and genetic (unpublished) work, which demonstrated that most residues that belong to the concave side of loop 2 are implicated in the toxin-receptor complex. Hence, it appears that loop 1 remains accessible from outside, in agreement with several arguments based on chemical modifications (2–5) or accessibility to large molecules (5, 14). In particular, there might still be enough space for the heavy chain of the Mα1 to bind to the loop 1 of the complexed toxin-α and then to destabilize the toxin-AcChoR complex, as postulated (9).

We are grateful to P. Fromageot and F. Kotzyba-Hibert for continuous interest and fruitful discussions and to Dr. C. Juret for building the computerized model. This investigation was supported in part by funds from the Ministère de l'Industrie et de la Recherche, the Centre National de la Recherche Scientifique, the Institut National de la Santé et de la Recherche Médicale, and the Commissariat à l'Energie Antomique. One of us (B.C.) received support from the Direction des Recherches, Etudes et Techniques.

1. Low, B. W. (1979) *Handb. Exp. Pharmacol.* **52,** 213–257.
2. Faure, G., Boulain, J. C., Bouet, F., Montenay-Garestier, T., Fromageot, P. & Ménez, A. (1983) *Biochemistry* **22,** 2068–2076.
3. Dufton, M. J. & Hider, R. C. (1983) *CRC Crit. Rev. Biochem.* **14,** 113–171.
4. Endo, T. & Tamiya, N. (1987) *Pharmacol. Ther.* **34,** 403–451.
5. Lobel, P., Kao, N. P., Birken, S. & Karlin, A. (1985) *J. Biol. Chem.* **260,** 10605–10612.
6. Trémeau, O., Boulain, J. C., Couderc, J., Fromageot, P. & Ménez, A. (1986) *FEBS Lett.* **208,** 236–240.
7. Garcia-Borron, J. C., Bieber, A. L. & Martinez-Carrion, M. (1987) *Biochemistry* **26,** 4295–4303.
8. Boulain, J. C., Ménez, A., Couderc, J., Faure, G., Liacopoulos, P. & Fromageot, P. (1982) *Biochemistry* **21,** 2910–2915.
9. Boulain, J. C. & Ménez, A. (1982) *Science* **217,** 732–733.
10. Rousselet, A., Faure, G., Boulain, J. C. & Ménez, A. (1984) *Eur. J. Biochem.* **140,** 31–37.
11. Low, B. W., Preston, H. S., Sato, A., Rosen, L. S., Searl, J. E., Rudko, A. D. & Richardson, J. S. (1976) *Proc. Natl. Acad. Sci. USA* **73,** 2991–2994.
12. Fryklund, L. & Eaker, D. (1975) *Biochemistry* **14,** 2865–2871.
13. Popot, J. L. & Changeux, J. P. (1984) *Physiol. Rev.* **64,** 1162–1239.
14. Ménez, A. (1985) *Pharmacol. Ther.* **30,** 91–113.
15. Saitoh, T., Oswald, R., Wennogle, L. & Changeux, J. P. (1980) *FEBS Lett.* **116,** 30–36.
16. Ishikawa, Y., Ménez, A., Hori, H., Yoshida, H. & Tamiya, N. (1977) *Toxicon* **15,** 477–488.
17. Laemmli, U. K. (1970) *Nature (London)* **227,** 680–685.
18. Porter, R. (1959) *Biochemistry* **73,** 119–123.
19. Neubig, R. R. & Cohen, J. B. (1979) *Biochemistry* **18,** 5464–5475.
20. Sine, S. M. & Taylor, P. (1981) *J. Biol. Chem.* **256,** 6692–6699.
21. Ratnam, M., Gullick, W., Spiess, J., Criado, M. & Lindstrom, J. (1986) *Biochemistry* **25,** 4268–4275.
22. Zeghloul, S., Marchot, P., Bougis, P. & Ronin, C. (1988) *Eur. J. Biochem.* **174,** 543–550.
23. Amit, A. G., Mariuzza, R. A., Phillips, S. E. V. & Poljack, R. J. (1986) *Science* **233,** 747–753.
24. Bayley, H. (1983) *Laboratory Techniques in Biochemistry and Molecular Biology*, eds. Work, T. S. & Burdon, R. H. (Elsevier, Amsterdam), Vol. 12.
25. Kubalek, E., Kalston, S., Lindstrom, J. & Unwin, P. N. T. (1987) *J. Cell Biol.* **105,** 9–18.
26. Langenbuch-Cachet, J., Bon, C., Mulle, C., Goeldner, M., Hirth, C. & Changeux, J. P. (1988) *Biochemistry* **27,** 2346–2357.
27. Tzartos, S. J. & Changeux, J. P. (1984) *J. Biol. Chem.* **259,** 11512–11519.
28. Witzemann, V., Muchmore, D. & Raftery, M. A. (1979) *Biochemistry* **18,** 5511–5518.
29. Hucho, F. (1979) *FEBS Lett.* **103,** 27–32.
30. Nathanson, N. M. & Hall, Z. W. (1980) *J. Biol. Chem.* **255,** 1698–1703.
31. Oswald, R. E. & Changeux, J. P. (1982) *FEBS Lett.* **139,** 225–229.
32. Hamilton, S. L., Pratt, D. R. & Eaton, D. C. (1985) *Biochemistry* **24,** 2210–2219.
33. Tsetlin, V., Plushnikov, K., Karelin, A. & Ivanov, V. (1983) in *Toxins as Tools in Neurochemistry*, eds. Hucho, F. & Ouchnikov, Y. A. (de Gruyter, Berlin), pp. 159–169.
34. Brisson, A. & Unwin, P. N. T. (1985) *Nature (London)* **315,** 474–477.